ELSEVIER

Chemical Physics 247 (1999) 155–162

Chemical Physics

www.elsevier.nl/locate/chemphys

Surface-enhanced non-linear Raman scattering at the single-molecule level

Katrin Kneipp [a,b,*], Harald Kneipp [a,b], Irving Itzkan [a,b], Ramachandra R. Dasari [a,b], Michael S. Feld [a,b]

[a] *G.R. Harrison Spectroscopy Laboratory, Massachusetts Institute of Technology, Cambridge, MA 02139, USA*
[b] *Physics Department, Technical University Berlin, D-10623 Berlin, Germany*

Received 28 January 1999

Abstract

Surface-enhanced hyper-Raman scattering and surface-enhanced anti-Stokes Raman scattering were studied as potential tools for non-linear single-molecule Raman spectroscopy. Experiments were performed using near-infrared excitation on crystal violet adsorbed on colloidal silver or gold clusters. Strong enhancement factors on the order of 10^{20} were inferred from hyper-Raman scattering experiments on colloidal silver. Such extremely high enhancement factors overcome the inherently weak nature of the effect, and surface-enhanced hyper-Raman scattering appears on comparable intensity levels as surface-enhanced Raman scattering. Surface-enhanced anti-Stokes Raman scattering starts from vibrational levels, that are populated by the very strong surface-enhanced Raman process. Thus, the anti-Stokes Raman scattering signal depends quadratically on the excitation laser intensity. For the first time, surface-enhanced anti-Stokes and Stokes Raman scattering was detected from single molecules on colloidal gold clusters.

1. Introduction

Optical spectroscopy of single molecules is an area of growing interest. Of particular importance are methods which can be applied under practical conditions, such as at room temperature and in liquids or on surfaces. One-photon excited fluorescence is the most prominent technique for single-molecule detection [1,2]. Two-photon fluorescence has been demonstrated to be a powerful tool for single-molecule detection in solution [3], or for monitoring single molecules on a surface [4]. Compared to one-photon fluorescence, the advantages for spectroscopic application of two-photon fluorescence are a confined probed volume, and signals which appear in a spectral range well separated from the excitation laser.

An important challenge to analytical chemistry is not only detecting a single molecule, but also identifying its chemical structure. In general, fluorescence spectroscopy at room temperature gives little information on the structure of a molecule. A Raman spectrum provides much structural information about the molecule and allows chemical identification. However, Raman scattering is a very weak effect and a large number of molecules is required to achieve adequate Raman signals.

This situation is dramatically altered for surface-enhanced Raman scattering (SERS). The phenomenon of a strongly increased Raman signal from molecules attached to metallic nanostructures was discovered in 1977 by Van Duyne, Jeanmaire, Al-

* Corresponding author. E-mail: kneipp@usa.net

0301-0104/99/$ - see front matter
PII: S0301-0104(99)00165-2

brecht and Creighton [5,6]. The enhancement mechanisms are roughly divided into 'electromagnetic' and 'chemical' effects. Chemical SERS enhancement is attributed to a metal electron mediated resonance Raman effect via a charge transfer intermediate state. The electromagnetic or field enhancement factor arises from enhanced laser and Raman fields due to electromagnetic resonances in the metallic structures [7,8]. As in 'normal' Raman scattering, surface-enhanced Raman scattering depends linearly on the excitation laser intensity.

In the electromagnetic field enhancement model, non-linear Raman effects such as hyper-Raman scattering are surface enhanced to a greater extent than 'normal' Raman scattering since they depend non-linearly on the laser field. This is confirmed by the very strong signals obtained in surface-enhanced hyper-Raman scattering experiments [9–11].

To use Raman scattering at the single-molecule level, the effective Raman cross-section has to be surface-enhanced about 14 orders of magnitude [12–16]. We obtained such extremely high enhancement factors at near-infrared (NIR) excitation for molecules adsorbed on colloidal silver [12–16] or gold clusters [17]. A very inhomogeneous field distribution on such clusters can result in extremely strong fields, which are confined in very small areas, the so-called 'hot spots' [18,19]. These strong fields then give rise to very high electromagnetic enhancement providing a rationale for such an extreme SERS effect. Hot spots imply particularly exciting perspectives for surface-enhanced non-linear optical phenomena as was theoretically demonstrated by Poliakov, Markel and Shalaev for second- and third-harmonic generation (SHG and THG, respectively), for degenerate four-wave mixing (DFWM), and for the optical Kerr effect [20].

In this study, we experimentally investigated surface-enhanced non-linear Raman processes, which should also benefit strongly from the extremely large field enhancements available in hot spots. Particularly, it might be challenging to apply non-linear Raman scattering to single molecules located in the hot spots. Surface-enhanced hyper-Raman scattering and 'pumped' anti-Stokes Raman scattering are selected as effects where the Raman scattering signal depends quadratically on the excitation laser intensity.

2. Experimental

Non-linear Raman effects are studied on colloidal silver or gold clusters, which are in aqueous solution or dried on a glass cover slide. Silver colloids are prepared from silver nitrate by citrate-reduction technique [21]. Colloidal gold solutions are used as commercially provided (Polysciences). NaCl was added in 10^{-2}–10^{-1} M concentration to the colloidal solutions to induce aggregation and to achieve the formation of colloidal clusters. The colloidal structures are characterized by extinction spectra of their aqueous solutions and by electron microscopy.

Crystal violet was selected as a target molecule. From its absorption spectrum [10], we conclude that only a very small molecular resonance Raman signal is expected to contribute to the observed total signal at the applied near-infrared excitation wavelength. Crystal violet is prepared as low-concentration solute in methanol and added to the colloidal solution resulting in final concentrations between 10^{-6} and 10^{-9} M in the target species.

The Raman systems for the surface-enhanced hyper-Raman experiments and for surface-enhanced anti-Stokes Raman spectroscopy are the same as described in previous papers [11,22].

In the hyper-Raman experiments the excitation source is an argon-ion laser pumped mode locked Ti:sapphire laser operating at 82 MHz with an average power of ~ 1 W. The excitation wavelength is tuned between 750 and 830 nm. The laser beam is focused into the sample to obtain a peak power density on the order of 10^{7}–10^{8} W/cm^2. The scattered light is collected at an angle of 90° relative to the incident laser beam and directed onto the entrance slit of the double grating monochromator. The Raman spectrum is recorded in a scanning regime using a photomultiplier tube for detection. To measure the SEHRS spectrum (shifted to the second harmonic of the NIR excitation), a NIR absorbing Schott filter is placed in front of the entrance slit of the monochromator. By removing this filter, the surface-enhanced Raman light and the surface-enhanced hyper-Raman light are measured simultaneously in the same spectrum using the first and second diffraction orders of the monochromator. This allows a direct determination of the ratio between SEHRS and SERS signal intensities. The relative

wavelength sensitivity of the system for Raman, as compared to hyper-Raman scattering was determined by using Raman spectra of benzene measured at NIR excitation and at the appropriate second-harmonic excitation [11].

Anti-Stokes Raman spectroscopy experiments were performed with 830 nm cw Ti:sapphire laser excitation at a power of $\sim$ 100 mW at the sample. A microscope is used for focusing excitation light and for collecting Raman scattered light in a 180° scattering geometry. Dispersion and detection of the scattered light is achieved using single grating spectrographs with deep depletion CCD detectors. Stokes- and anti-Stokes spectra are collected in 1 s.

Collection volumes are on the order of μl in the hyper-Raman experiments. By using a confocal Raman microscope in the anti-Stokes Raman experiments, the probed volumes are $\sim$ 1 fl.

3. Results and discussion

3.1. Colloidal gold and silver clusters

Fig. 1a shows extinction spectra of the colloidal gold and silver cluster structures used in the experiments. The broad extinction curve, which extends into the near-infrared region is an indication of the formation of relatively large clusters [10,17]. Fig. 1b shows an electron microscope view of a typical colloidal silver cluster with a μm dimension. Colloidal gold shows very similar aggregation behavior and cluster formation [23,24]. From surface-enhanced Raman experiments performed using colloidal gold and silver cluster structures, we know, that these clusters can provide extremely high enhancement level, on the order of 10^{14}, in linear surface-enhanced Raman scattering experiments [12–17]. After exceeding a critical size dimension, SERS enhancement factors are found to be independent of the size of colloidal clusters [16,17]. Colloidal gold clusters, which represent about the required minimum cluster size are displayed in Fig. 1c.

In order to make the large enhancement factors consistent with the level of the observed SERS Stokes signal, we must conclude that only a very small fraction of target molecules available in the sample are involved in the Raman process at the extremely high enhancement level and contribute to the measured SERS spectrum [12]. This experimental finding might be explained by the existence of hot spots in the cluster structures [18–20]. Only a small fraction of the molecules in the sample can find a place at such hot zones and can 'feel' the extreme field enhancement.

In the following, these colloidal structures are studied in non-linear Raman experiments.

3.2. Surface-enhanced hyper-Raman scattering (SEHRS)

Hyper-Raman scattering (HRS) results in a scattering signal that is Raman shifted relative to the second harmonic of the excitation frequency, and that depends quadratically on the excitation intensity (for an overview, see Ref. [25]). For molecules having high symmetry, hyper-Raman spectra can provide vibrational information on so-called 'silent modes' which cannot be obtained using 'normal' Raman scattering (RS) or infrared absorption spectroscopy. Since HRS has a very low cross-section, the effect has not been used in practical spectroscopic applications.

Strong surface enhancement factors can overcome the inherently weak nature of hyper-Raman scattering and surface-enhanced hyper-Raman spectra have been measured at relatively low excitation intensities for several molecules ([11] and references therein).

Fig. 2a displays a portion of the hyper-Raman spectrum of 10^{-8} M crystal violet on colloidal silver clusters measured at different excitation wavelengths. From surface-enhanced Raman experiments we know, that target molecules are involved in the Raman process at extremely large enhancement level only in $\sim 10^{-12}$ M concentration [12]. We are using so many excess molecules to make sure that – wherever a 'hot spot' might be generated for the different excitation wave lengths – a target molecule will be available to probe the field by an enhanced Raman process.

The hyper-Raman signal strongly increases with increasing excitation wavelength. No hyper-Raman spectrum could be measured at 750 nm excitation. This can be explained with a 'field enhancement model' where the total enhancement benefits from

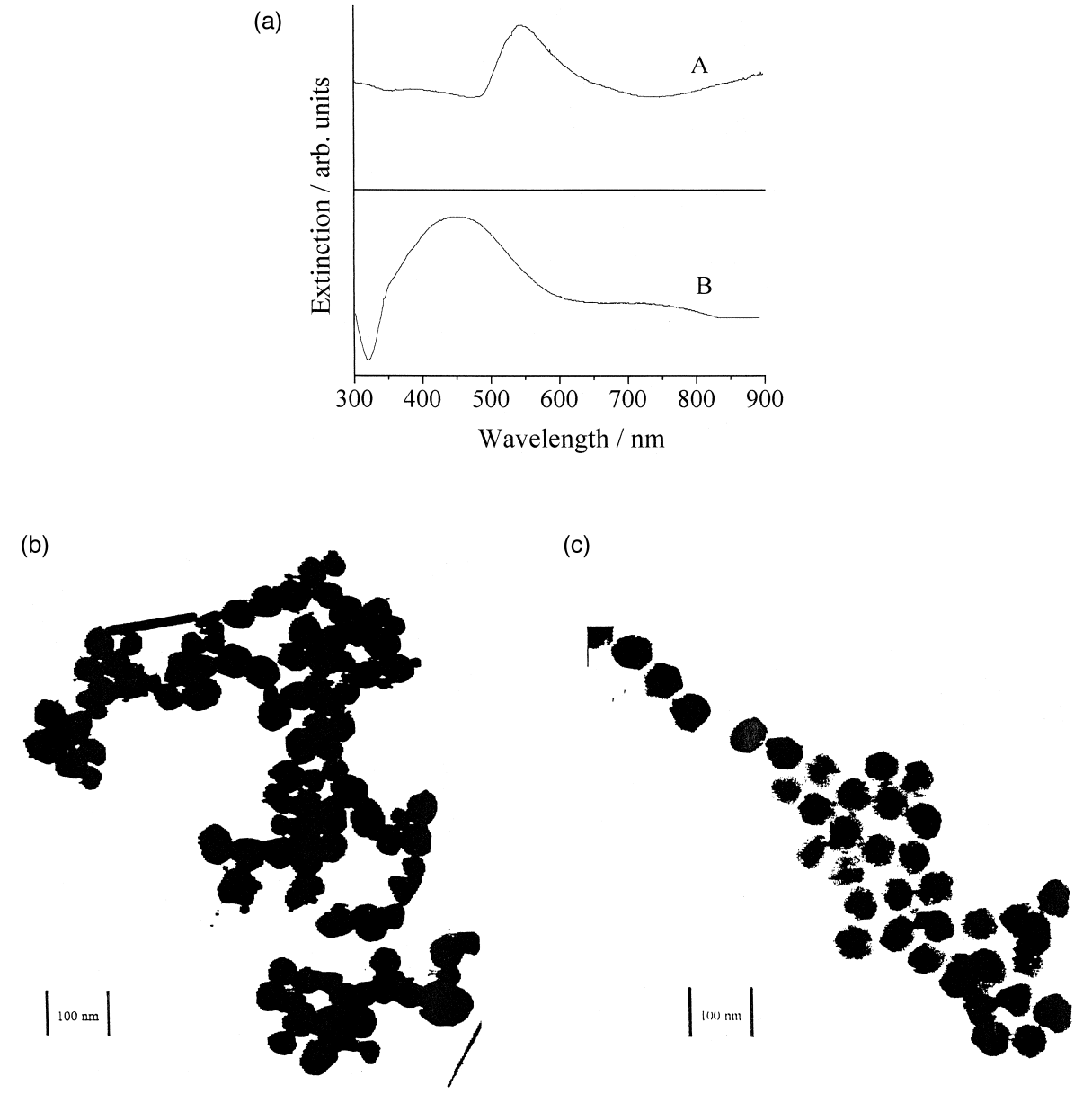

Fig. 1. (a) Extinction spectra of the aqueous solutions of the applied colloidal gold (A) and silver (B) clusters. (b) Electron microscopic view of typical colloidal silver cluster structure. (c) Electron microscopic view of typical colloidal gold cluster.

enhancement of laser *and* scattering field. At 750 nm excitation, the hyper-Raman Stokes field wavelength is too short to benefit from any resonances with the colloidal silver. This missing enhancement for the scattering field reduces the total enhancement to a level which is not sufficient to compensate for the extreme weakness of the hyper-Raman effect. This situation is altered at 785 nm and longer excitation wavelengths. In general, the field confinement will become more pronounced at longer excitation wavelengths [20] in agreement with our experimental observation of increasing hyper-Raman signals.

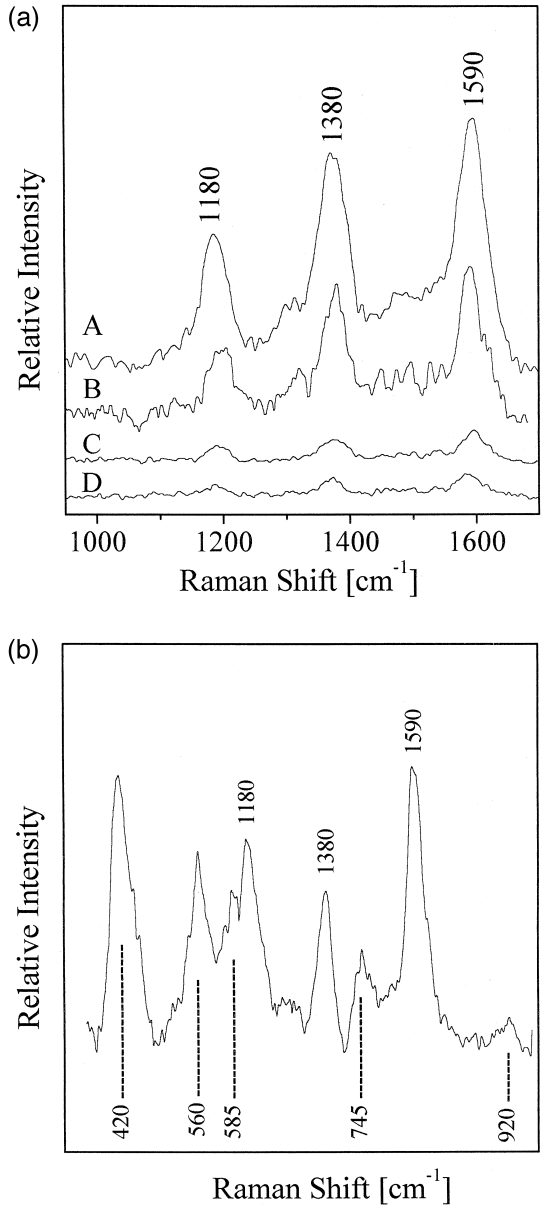

Fig. 2. (a) Surface-enhanced hyper-Raman bands of crystal violet measured on colloidal silver clusters at: 833 nm (A), 815 nm (B), 798 nm (C), and 785 nm (D) excitation wavelength. (b) Surface-enhanced hyper-Raman bands (wave numbers on the top) and surface-enhanced Raman bands (wave numbers below) of crystal violet measured on colloidal silver cluster at 805 nm excitation.

Fig. 2b shows surface-enhanced hyper-Raman and Raman scattering signals added together in the same spectrum. The Raman wave numbers and relative intensities of SERS and SEHRS lines in the crystal violet spectrum are in agreement with previously published spectra of this molecule on silver colloids [10,11]. The appearance of surface-enhanced hyper-Raman and Raman scattering at the same signal intensity [1] suggests that surface-enhanced hyper-Raman scattering is a spectroscopic technique that can be applied at single-molecule level.

As described in Ref. [11], the experimental ratios between SERS and SEHRS intensities can be combined with the corresponding estimated 'bulk' intensity ratio between Raman scattering and hyper-Raman scattering for the applied 10^7 W/cm^2 excitation intensity to infer a ratio between surface-enhancement factors of hyper-Raman scattering and Raman scattering of $\sim 10^6$. Combining this ratio with NIR-SERS enhancement factors for crystal violet on the order of 10^{14} [12,13] total surface enhancement factors of hyper-Raman scattering on crystal violet adsorbed on colloidal silver clusters can be inferred to be on the order of 10^{20}.

Note that this enhancement can include electromagnetic and chemical contributions.

However, the experimental finding that extremely large enhancement at near-infrared excitation was obtained on colloidal clusters and has not been observed for non-aggregated silver or gold colloids [16,17] is an important indication that the electromagnetic field enhancement effect dominates.

3.3. Surface-enhanced anti-Stokes Raman scattering

As another non-linear Raman method, we studied surface-enhanced anti-Stokes Raman scattering. In surface-enhanced anti-Stokes Raman scattering, the increased population of the first excited vibrational states due to an extremely strong Raman process results in an increase of the anti-Stokes signal [12]. At relatively low excitation intensities (weakly saturating intensity regime $[\exp(-h\nu_m/kT) \leq \sigma^{SERS}(\nu_m)\tau_1(\nu_m)n_L \ll 1]$ as in our experiments), the anti-Stokes signal, P_a, depends quadratically on the

[1] Accounting for the different sensitivity of the detection system in the Raman and hyper-Raman region, the SERS intensity is stronger than the SEHRS intensity by about two orders of magnitude.

excitation intensity, whereas the Stokes signal, P_s, remains linearly dependent [12]:

$$P_a \approx \left[N_0 \exp\left(-\frac{h\nu_m}{kT} \right) + N_0 \sigma^{SERS} \tau_1 n_L \right] \sigma^{SERS} n_L \,, \quad (1a)$$

$$P_s \approx N_0 \sigma^{SERS} n_L \,, \quad (1b)$$

where N_0 is the number of molecules in the vibrational ground state, n_L is the laser intensity, σ^{SERS} and τ_1 are the effective SERS cross- section and the lifetime of the first excited vibrational state of a molecular vibration u_M, respectively, and T is the temperature of the sample. Fig. 3a shows the plots of the 1174 cm^{-1} anti-Stokes and Stokes SERS signals of crystal violet on colloidal gold clusters for different excitation intensities. The lines indicate quadratic and linear fits to the respective data, displaying the predicted dependence.

Fig. 3b shows SERS spectra of crystal violet on colloidal gold clusters measured at the anti-Stokes side of the 830 nm cw excitation laser. The 1174 cm^{-1} anti-Stokes line in curve A appears at ~ 20 times lower intensity compared to the appropriate Stokes line. (Surface-enhanced Stokes spectra of crystal violet on colloidal gold clusters are shown in Ref. [17].) Methanol anti-Stokes signals are not detected under these experimental conditions. As Fig. 3b shows, the anti-Stokes spectra appear at the Rayleigh background which is suppressed by a notch filter up to ~ 900 cm^{-1}. Due to the quadratic dependence of the anti-Stokes signal, the signal to background ratio is improved for increasing excitation laser intensities.

Fig. 4 shows anti-Stokes and Stokes SERS spectra of 10^{-9} M crystal violet in solution of colloidal gold clusters measured in 1 s collection time. Based on a concentration volume estimate, an average of about one molecule contributes to the spectra collected from ~ 1 fl probed volume. This is the first demonstration of single-molecule sensitivity in a SERS experiment performed on colloidal gold. The relative strong band at 1620 cm^{-1} in the anti-Stokes spectrum is an indication that the anti-Stokes signal arises from pumped vibrational levels and not from thermally populated ones. In the anti-Stokes spectrum the single-molecule lines appear at a signal to noise level of about 2:1. Fig. 4b shows the statistical

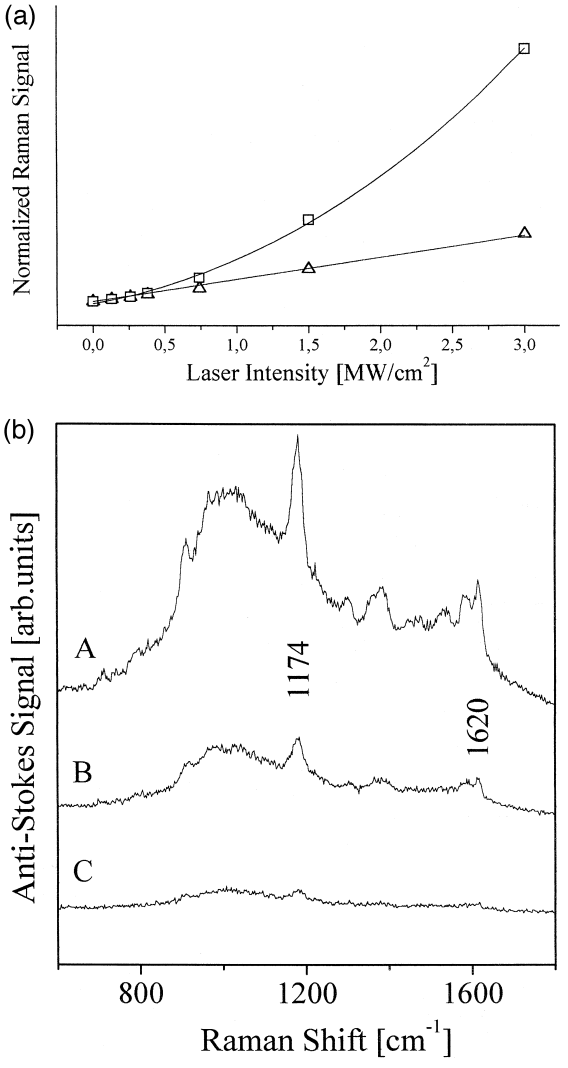

Fig. 3. (a) Surface-enhanced Stokes (△) and anti-Stokes (□) Raman scattering signal as a function of cw excitation intensity at 830 nm. (b) Surface-enhanced anti-Stokes Raman scattering of crystal violet on colloidal gold clusters at: 3 MW/cm^2 (A), 1.4 MW/cm^2 (B), and 0.7 MW/cm^2 (C) cw excitation intensities. The 1174 cm^{-1} Raman signal is increased compared to the Rayleigh background from (C) to (A).

distribution of the signals of 100 anti-Stokes measurements. The anti-Stokes Raman signals measured in time sequence were selected in 10 bins whose widths are 10% of the maximum of the observed signals (x-axis). The y-axis displays the frequency of the appearance of the appropriate signal levels of the bin. All signals at 10% level of the maximum

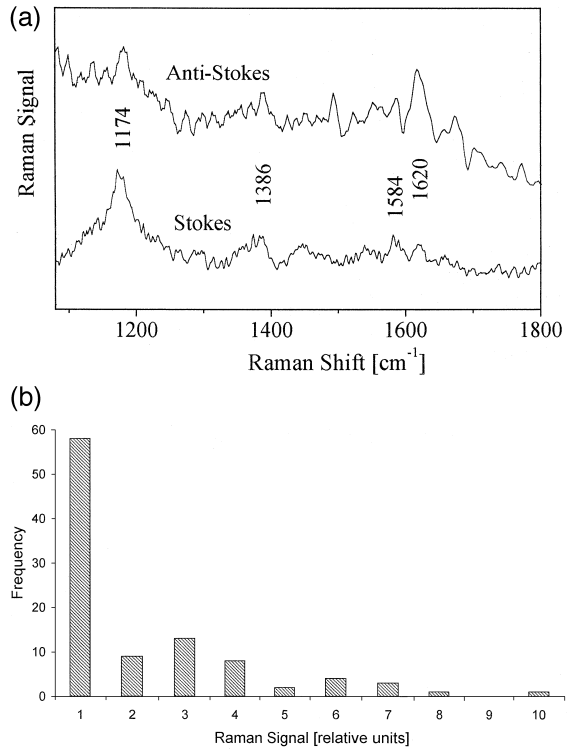

Fig. 4. (a) Surface-enhanced Stokes and anti-Stokes Raman scattering of single crystal violet molecules measured on colloidal gold clusters at 830 nm excitation wavelength in 1 s collection time. For assignment of bands, see also Fig. 3b and Ref. [17] where about 100–1000 crystal violet molecules contribute to the anti-Stokes and Stokes spectrum, respectively. (b) Statistical distribution of the anti-Stokes SERS signal at 1174 cm^{-1}. The peaks centered at the relative intensities 1, 3, and 6 reflect the probability to find just 0, 1, and 2 molecules in the scattering volume during the actual measurement, respectively.

intensity and lower were collected in bin '1' representing zero molecules in the probed volume. The statistical distribution of the anti-Stokes Raman signals shows a clear change from Gaussian, expected for 'many' molecules [13,15], to Poisson when the average number of analyte molecules in the scattering volume is one or fewer. As the signal distribution in Fig. 4b shows, ~ 60, ~ 30, and ~ 10 measurements indicate zero, one, and two molecules in the probed volume, respectively. These numbers are roughly consistent with a Poisson distribution for an average number of 0.5 molecule in approximate agreement with the above concentration/volume estimates.

4. Summary

Surface-enhanced hyper-Raman scattering and surface-enhanced anti-Stokes Raman scattering from pumped vibrational levels were studied as Raman processes where the scattering signal depends nonlinearly on the excitation laser intensity.

Both effects are observed on colloidal gold or silver clusters at near-infrared excitation and seem to benefit from extremely large field enhancements predicted for such cluster structures in so-called 'hot spots'.

Surface-enhanced hyper-Raman scattering benefits from an enhancement factor of ~ 20 orders of magnitude and can appear at comparable intensity levels as surface-enhanced Raman scattering. This provides hope that the effect can be successfully applied for single-molecule spectroscopy.

Due to the population of the first excited vibrational state in a strong Raman process, the surface-enhanced anti-Stokes signal shows a quadratic dependence on excitation laser intensity. Single crystal violet molecules on colloidal gold clusters can be detected by their surface-enhanced Raman signal at the anti-Stokes side of the near-infrared excitation laser.

5. Uncited reference

[26]

References

[1] R. Keller, W.P. Ambrose, P.M. Goodwin, J.H. Jett, J.C. Martin, M. Wu, Appl. Spectrosc. 50 (1996) 12A.
[2] R. Rigler, J. Widengren, Ü. Mets, in: O.S. Wolfbeis (Ed.), Fluorescence Spectroscopy, Springer, Berlin, 1992, p.13.
[3] J. Mertz, C. Xu, W.W. Webb, Opt. Lett. 20 (1995) 2532.
[4] E.J. Sanchez, L. Novotny, G.R. Holtom, X.S. Xie, Phys. Chem. A 101 (1997) 7019.
[5] D.L. Jeanmaire, R.P. Van Duyne, J. Electroanal. Chem. 84 (1977) 1.
[6] M.G. Albrecht, J.A. Creighton, J. Am. Chem. Soc. 99 (1977) 5215.
[7] A. Otto, in: M. Cardona, G. Guentherodt (Eds.), Light Scattering in Solids, Springer, Berlin, 1984, p.289.
[8] M. Moskovits, Rev. Mod. Phys. 57 (1985) 783.
[9] C.K. Johnson, S.A. Soper, J. Phys. Chem. 93 (1989) 7281.

[10] H. Kneipp, K. Kneipp, F. Seifert, Chem. Phys. Lett. 212 (1993) 374.
[11] K. Kneipp, H. Kneipp, F. Seifert, Chem. Phys. Lett. 233 (1995) 519.
[12] K. Kneipp, Y. Wang, H. Kneipp, I. Itzkan, R.R. Dasari, M.S. Feld, Phys. Rev. Lett. 76 (1996) 2444.
[13] Kneipp, Y. Wang, H. Kneipp, L.T. Perelman, I. Itzkan, R.R. Dasari, M.S. Feld, Phys. Rev. Lett. 78 (1997) 1667.
[14] S. Nie, S.R. Emory, Science 275 (1997) 1102.
[15] K. Kneipp, H. Kneipp, G. Deinum, I. Itzkan, R.R. Dasari, M.S. Feld, Appl. Spectrosc. 52 (1998) 175.
[16] K. Kneipp, H. Kneipp, V.B. Kartha, R. Manoharan, G. Deinum, I. Itzkan, R.R. Dasari, M.S. Feld, Phys. Rev. E 57 (1998) R6281.
[17] K. Kneipp, H. Kneipp, E.B. Hanlon, I. Itzkan, R.R. Dasari, M.S. Feld, Appl. Spectrosc. 52 (1998) 1493.
[18] V.M. Shalaev, Phys. Rep. 272 (1996) 61.
[19] M. Stockman, V.M. Shalaev, M. Moskovits, R. Botet, T.F. George, Phys. Rev. B 46 (1992) 2821.
[20] E.Y. Poliakov, V.A. Markel, V.M. Shalaev, R. Botet, Phys. Rev. B 57 (1998) 14901.
[21] P.C. Lee, D.J. Meisel, Phys. Chem. 86 (1982) 3391.
[22] K. Kneipp, H. Kneipp, R. Manoharan, I. Itzkan, R.R. Dasari, M.S. Feld, Bioimaging 6 (1998) 104.
[23] D.A. Weitz, M. Oliveria, Phys. Rev. Lett. 52 (1984) 1433.
[24] K. Güldner, R. Liedtke, K. Kneipp, H.J. Eichler, Europhysics Conference Abstracts, 29th EGAS, Berlin, Eur. Phys. Soc., Petit-Lancy, 1997, p.128.
[25] L.D. Ziegler, J. Raman Spectrosc. 21 (1990) 769.
[26] K. Kneipp, H. Kneipp, R. Manoharan, I. Itzkan, R.R. Dasari, M.S. Feld, J. Raman Spectrosc. 29 (1998) 743.